

Quantitative and qualitative analysis of a microfluidic DNA extraction system using a nanoporous AlO_x membrane

Jungkyu Kim^a and Bruce K. Gale^{*b}

Received 19th March 2008, Accepted 3rd June 2008

First published as an Advance Article on the web 17th July 2008

DOI: 10.1039/b804624g

A nanoporous aluminium oxide membrane was integrated into a microfluidic system designed to extract hgDNA (human genomic DNA) from lysed whole blood. The effectiveness of this extraction system was determined by passing known concentrations of purified hgDNA through nanoporous membranes with varying pore sizes and measuring the amount of hgDNA deposited on the membrane while also varying salt concentration in the solution. DNA extraction efficiency increased as the salt concentration increased and nanopore size decreased. Based on these results, hgDNA was extracted from whole blood while varying salt concentration, nanopore size and elution buffer to find the conditions that yield the maximum concentration of hgDNA. The optimal conditions were found to be using a low-salt lysis solution, 100 nm pores, and a cationic elution buffer. Under these conditions the combination of flow and ionic disruption were sufficient to elute the hgDNA from the membrane. The extracted hgDNA sample was analysed and evaluated using PCR (polymerase chain reaction) to determine whether the eluted sample contained PCR inhibition factors. Eluted samples from the microfluidic system were amplified without any inhibition effects. PCR using extracted samples was demonstrated for several genes of interest. This microfluidic DNA extraction system based on embedded membranes will reduce the time, space and reagents needed for DNA analysis in microfluidic systems and will prove valuable for sample preparation in lab-on-a-chip applications.

Introduction

As micro/nanofabrication technologies are developed, researchers in the biological and medical fields are adopting these technologies to miniaturize complicated and time consuming assays. As most biological samples come in a liquid form, micro/nanofluidics is the most applicable method for miniaturized instrumentation. As a result of these research efforts, μ -TAS (micro total analysis systems) have been realized and used for biological sample analyses, chemical reactions, and diagnostics. In particular, there is significant worldwide interest in developing microfluidic systems for point-of-care diagnostics. In most cases, DNA diagnostics involves three steps: sample preparation, amplification and detection. The ability to process raw samples and subsequently perform the required analytical operations on-chip is key to the eventual success of DNA-focused microfluidic systems. Sample preparation takes time to complete inside miniaturized systems and can be difficult to integrate with PCR (polymerase chain reaction) or other analysis/detection methods. When a DNA sample is isolated from whole blood or a similar sample, one has to remove proteins and other materials that inhibit PCR or other analysis techniques. A variety of techniques have been developed to

perform this DNA extraction from biological samples including methods involving: static silica pillars or beads (standard solid-phase extraction techniques), magnetic silica particles, chitosan-coated surfaces, micro/nanopillar sieves, and nanoporous membranes.^{1–15} Micro-solid phase extraction (μ SPE) is typically used to prepare DNA samples for genetic analysis within microchips. Microchannels containing silica resin have been shown to be effective for the adsorption and desorption of DNA in chaotropic salt solution.¹ As techniques using silica bead and silica particles immobilized in sol-gels are examined, the best results obtained use a silica particle/sol-gel hybrid. In that research, they examined the performance of sol-gel-immobilized silica particles in a microchannel for purification of DNA on a microchip SPE device.^{2,3,13} Another group used a similar concept by microfabricating channels in which silica-coated pillars were etched to increase the surface area within the channel by 300–600%.⁴ The micropillars significantly increased the efficiency of DNA extraction. Surface modified magnetic beads have also been used to increase the DNA yield.^{5,6} Extraction techniques based on other electrostatic interactions with DNA have been demonstrated. The most basic include an amine surface coating. Amine groups have a positive charge below neutral pH (causing negatively charged DNA to bind) and the charge decreases above neutral pH. However, this method can affect the DNA amplification step due to the high pH required for elution.⁷ To overcome this pH problem associated with electrostatic methods, a chitosan surface coating was used to extract DNA from whole blood. Chitosan has a cationic charge at pH 5 and is easily neutralized at pH 9.

^aDepartment of Bioengineering, University of Utah, Salt Lake City, UT 84112, USA. E-mail: jungkyu.kim@utah.edu; Fax: +1 801-585-9826; Tel: +1 801-585-3176

^bDepartment of Mechanical Engineering, University of Utah, Salt Lake City, UT 84112, USA. E-mail: bruce.gale@utah.edu; Fax: +1 801-585-9826; Tel: +1 801-585-3176

High density microfluidic channels coated with chitosan were fabricated and tested with lysed whole blood samples. DNA was captured at pH 5.0 through electrostatic interaction and eluted using pH 9.1 Tris buffer. The recovery rate was found to be 68% for human genomic DNA.⁸ PCR (polymerase chain reaction) was demonstrated with the eluted DNA. Variations on solid phase extraction, where mobile magnetic beads are used to spatially separate bound DNA after binding has been completed, have been demonstrated. Magnetic beads with amine groups on the surface have been implemented to increase the DNA binding affinity. To simplify the surface modification process and maximize the release ratio of DNA, aminosilane modification techniques and an optimized buffer were used to improve the DNA extraction and elution efficiency.⁹ Like other electrostatic methods, the capture and release efficiency was influenced by the protein content. Negatively charged protein may interact with positively charged magnetic beads, decreasing the efficiency of DNA extraction. A combination of sieving and electrostatic interactions to improve DNA yield has also been proven useful. For example, a microfluidic DNA extraction system with a nanoporous membrane was proposed and tested with λ -DNA. This work was based on earlier work showing that aluminium oxide membranes could be used to extract DNA.^{10–12}

While there have been several techniques for DNA extraction demonstrated, most of the methods suffer from manufacturing complexity, either in the lithography processes or during assembly (loading) after the microfluidic system has been built. The DNA yield for many of these techniques is also relatively low. Some of these techniques are also not readily compatible with some standard microfluidic techniques, such as soft lithography. Thus, as reported in this paper, a microfluidic system integrated with a nanoporous aluminium oxide membrane was developed that can both simplify fabrication and generate a high DNA yield. These nanoporous aluminium oxide membranes have been demonstrated for DNA extraction, have low protein absorption, allow a high flow rate, and have a regular pore pattern.^{11,12} However, these membranes are difficult to integrate into a microfluidic system since they are very brittle. To find the optimal physical and chemical conditions for DNA extraction, three nanopore sizes and salt concentrations were tested and evaluated for DNA extraction. The rationale for using nano-filtration is that gDNA in whole blood is a large macromolecule compared to other components in blood, suggesting that gDNA can be separated by size. Decreasing the nanopore size and increasing the salt concentration causes the DNA to aggregate and thus adsorption onto the nanoporous structure is increased. After capture of the gDNA, appropriate wash buffer concentrations and pH levels are needed to maximize the DNA recovery rate. After extracting gDNA from human blood using the aluminium oxide membrane, DNA amplification was performed using a real-time PCR instrument. The level of PCR inhibition factors was estimated from serially diluted PCR experiments.

Materials and methods

Materials and microdevice fabrication

Previous work in our lab has demonstrated a technique for integrating the nanoporous aluminium oxide membranes (AOM)

into a microfluidic system,^{10,11} though significant new advances are presented here. The AOMs (distributed by Whatman, Inc., UK) were used as the surface for hgDNA sample extraction and preparation and integrated into the microfluidics. Three different pore sizes, 20 nm, 100 nm and 200 nm, were available from the manufacturer. The AOMs are relatively inert biologically, rigid at the microscale, and have low autofluorescence. Their high porosity (50%) allows for high flow rates through the membrane.¹⁶ The microfluidics were fabricated using polydimethylsiloxane (PDMS) soft lithography and an SU-8 mold on a 75 mm silicon wafer. Two nearly identical copies of the PDMS microfluidics were generated and the AOM for extraction bonded between the two microfluidic sections as shown in Fig. 1. To make the soft lithography mold, the mold wafer was heated for 5 min at 200 °C and SU-8 50 (MicroChem Corp., Newton, MA, USA) was spun on at 1300 rpm for 30 s to produce a 100 μ m thick layer. The SU-8 was soft-baked at 65 °C for 3 min and 95 °C for 2.5 h to remove any solvent and then exposed at 365 nm with a EV-420 aligner (Electronic Visions Inc., Tempe, AZ, USA). The post exposure bake was carried out for 3 min at 65 °C for 2 min and 95 °C for 5 min to complete the crosslinking of the exposed structures. The wafer was developed in PGMEA (propylene glycol monomethyl ether acetate) from MicroChem with gentle shaking for 7 min, washed with isopropyl alcohol, and dried with a nitrogen spray. To prevent the cured, molded PDMS from bonding to the native oxide present on the patterned silicon wafer, a fluorosilane compound (Gelest Inc., Morrisville, PA, USA) was vapor-deposited onto the wafer in a vacuum chamber for 1 h prior to casting the PDMS mold. The mold was then ready for PDMS patterning.

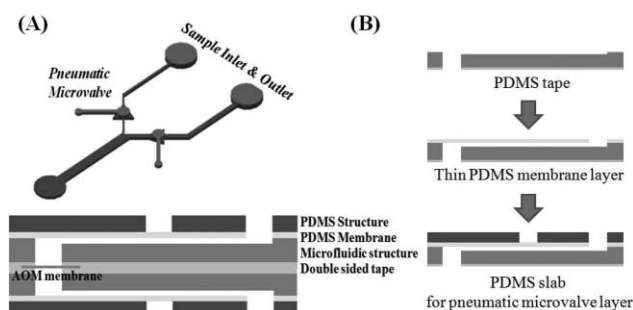


Fig. 1 Design of the nanoporous membrane-embedded microfluidic gDNA extraction system. The microfluidic channels and the microvalve were fabricated with soft lithography. Details of the process are included in the text. (A) The channel layout of the microfluidic control system. (B) Cross sectional view of the fabrication process.

The critical fabrication step in this work was to integrate the nanoporous membrane with the microfluidics. To accomplish this task, the microfluidic layers need to be bonded to the membrane. The nanoporous membranes do not bond well with PDMS, even though surface activation methods such as oxygen plasma or corona discharge were used. As an alternative to these plasma/corona bonding methods, we developed a unique method based on xurography technologies,¹⁷ which use cut double-sided tapes to form the microfluidic channels. To provide a good bonding surface, double sided tape was integrated with the PDMS during the curing process. Liquid PDMS was used as provided from the manufacturer (Sylgard 184®, Dow Corning,

WI), with a base resin to curing agent ratio of 10 : 1. The mixed PDMS was placed in a vacuum chamber for 30 min to remove any air bubbles, poured over double sided tape, (3M™ Double Coated Tape 444, 3M Corp., MN) placed at the bottom of a Petri dish, and then covered with the SU-8 mold. After removing air from the molded PDMS in a vacuum chamber, it was placed in a 65 °C oven for 45 min to cure. After the cure was complete, the casting was peeled from the mold. The final cast had microfluidic channels on the top side and the double-sided tape bonded to bottom of the PDMS cast : tape embedded microfluidic system (Fig. 1). A hole for the sample to flow through the AOM was made using a coring tool.¹⁸ The backing tape was removed and the membrane was sandwiched between the PDMS/tape microfluidic structures. To control the direction of flow in the microchannels, a membrane microvalve was fabricated and integrated with the membrane embedded system, as shown in Fig. 1. To implement the pneumatic microvalve, a thin PDMS layer was spin coated over a 75 mm wafer at 3000 rpm for 30 s. The wafer was partially cured for 30 min in an oven at 65 °C. The partially cured PDMS membrane and the tape-embedded microfluidic structure described previously were then clamped together and cured at 65 °C for 30 min. After curing for 30 min, the wafer supporting the membrane was peeled off and the PDMS membrane was transferred and bonded to the microfluidic structure. To connect tubing for the inlet ports, outlet ports, and membrane valve control, the top, flat PDMS layer was cored and then bonded with the tape-embedded microfluidic system using the oxygen plasma method.^{19,20} The nanoporous membrane was then inserted between two of these constructs, with the double sided tape being exposed to form the bond. To improve bond strength, the integrated microfluidic structure was clamped and put into a 65 °C oven for 2 h. The final system aligned and stacked with the flat PDMS, the thin PDMS membrane, the PDMS microchannel layer, and the aluminium oxide membrane, respectively, from top to bottom is shown in Fig. 2 under a light field microscope.

Experimental

Nanopore size and salt concentration effect

Physical DNA filtration, based on different processing conditions, was evaluated using three different nanopore sizes and three salt concentrations. The hgDNA purified from human blood is a macromolecule and can be physically captured with the nanoporous filters, and can be electrostatically captured using the charge on the AOM. To optimize DNA extraction using these nanopore membranes, there is a need to determine the optimal pore size for DNA extraction. Furthermore, the optimal pore size may vary depending on the folded size and shape of the DNA, which can be controlled by changing the salt concentration. Thus, by managing the salt concentration, we hypothesize that the collection rate of DNA can be increased. To determine the nanopore size effect, the integrated microfluidic chip was made with membranes that have different pore sizes (20 nm, 100 nm, 200 nm). The hgDNA sample was also prepared with different salt concentrations (0, 100 mM, 300 mM and 500 mM NaCl) to determine the effect of varying salt concentrations.^{21,22} Samples containing approximately 500 ng

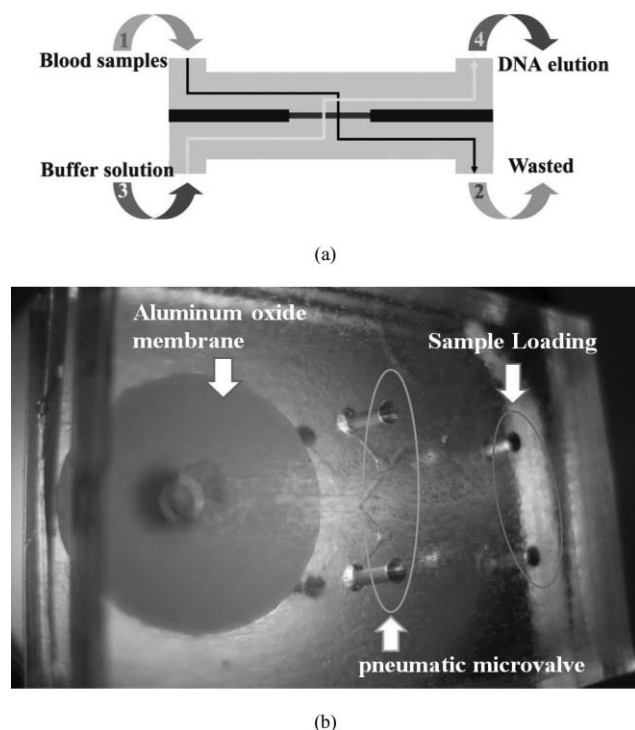


Fig. 2 (a) Experimental schematic of the DNA sample preparation system. Blood samples (1) pass through the membrane and DNA collects on the membrane as the other components are passed to waste (2). Then, the buffer solution (3) flows through microfluidic channels and elutes the gDNA that was collected on the AOM from the blood samples. The DNA is removed through outlet (4) or it can be connected directly to the next system. (b) Photograph of the microfluidic DNA extraction system integrated with the nanoporous membrane (aluminium oxide membrane: 13 mm diameter).

of gDNA (10 ng μl^{-1} concentration) were passed through the microsystems at 6.67 $\mu\text{l min}^{-1}$ using a syringe pump (KD scientific Inc., MA, USA). Usually, to complete the microfluidic system, oxygen plasma treatment is used for bonding PDMS to PDMS. After this treatment, the PDMS surface was deprotonated (SiO^-) and most of the gDNA flowed through the PDMS microfluidic channel without loss or adsorption problems.^{19,23} The amount of gDNA in the waste solution was measured using a spectrometer (Nanodrop N-100), therefore providing the amount of gDNA left captured on the membrane. Results relating pore size (20 nm, 100 nm, 200 nm) with salt concentration and gDNA captured were obtained by spectrometry.

DNA extraction from whole blood

The hgDNA embedded nanoporous membrane extraction system was tested with whole blood samples to evaluate the functionality of this chip with a real sample. The whole blood sample for the hgDNA extraction test was drawn with a finger-prick tool from a healthy volunteer. The test samples were prepared by mixing whole blood with 1% Triton X-100 for cell lysis, protease K (Sigma, Inc) for deactivating and breaking down the protein, sodium chloride (NaCl), and DI water. Total sample volume was 400 μl : 20 μl of blood, 160 μl of 1% Triton X, 20 μl of Protease K and 200 μl of DI water. When adding salt, 10 μl of 1 M NaCl was mixed with the sample instead of

10 μl of DI water. The 100 μl of lysed blood samples were passed through the microfluidic system with a $6.7 \mu\text{l min}^{-1}$ flow rate at room temperature. For elution of the hgDNA, 25 μl of two different ionic buffers, Tris-KCl buffer solution with pH 9 and a 5 mM phosphate buffer solution with pH 9, were flowed through the system in the reverse direction to elute the extracted DNA from the membrane.

Evaluation of extracted DNA sample

When measuring the quantity of DNA captured using real samples, a spectrophotometer is difficult to use because it can be challenging to obtain a consistent background. To overcome this problem, real-time PCR (polymerase chain reaction) was performed with the eluted DNA sample to determine the amount of DNA in the initial sample. The PCR mixture used for amplification consisted of 0.5 μM of each primer, 200 mM of each deoxynucleotide triphosphate (dNTP), 0.4 U of KlenTaq1 polymerase (AB Peptides, MO, USA), 88 ng of TaqStart antibody (ClonTech, CA, USA), 3 mM MgCl_2 , and 1X LC Green Plus (Idaho Technology, UT, USA) in 50 mM Tris (pH 8.3) and 250 ng ml^{-1} bovine serum albumin (BSA). With this mixture, the samples were loaded into capillary tubes and PCR was performed in a LightcyclerTM (Roche Inc, Indianapolis, IN) with the following conditions: initial denaturation at 95 $^{\circ}\text{C}$ for 15 s followed by 45 cycles of 95 $^{\circ}\text{C}$ for 0 s, 60 $^{\circ}\text{C}$ for 0 s, and 74 $^{\circ}\text{C}$ for 8 s. The temperature transition rate for all steps was 20 $^{\circ}\text{C s}^{-1}$. Amplification was performed with a 122 bp amplicon of the CYP2C9*2 gene using forward primer 5'-GAATTTTGGGATGGGGAAGAG-3' (21 bp) and reverse primer 5'-TCCAGTAAGGTCAGTGATATGG-3' (22 bp) and a 190 bp amplicon of the VKORC1 C1173T gene using forward primer 5'-GGGGAGGATAGGGTCAGT-3' (18 bp) and reverse primer 5'-GGTGAACAGGTTAGGAC-3' (19 bp). To validate the amplification, negative controls (without template DNA) were also amplified to ascertain whether the resulting amplicon is a product of residual contamination. After finishing the PCR step, DNA melt data was obtained with a Lightcycler, melting at a rate of 0.3 $^{\circ}\text{C s}^{-1}$. The extracted DNA concentration and quality is estimated using the PCR results and the melt curve. To measure the impact of inhibition factors in the extracted gDNA samples, extracted DNA samples using a commercial kit were mixed with amounts of gDNA extracted from the microchip. 10 μl of purified gDNA (10 $\text{ng } \mu\text{l}^{-1}$) was blended with 1 μl from the microchip and then PCR was performed with the LightcyclerTM. Comparing crossing points of the PCR profile allowed the inhibition effect of DNA samples extracted using the microchip to be estimated.

Results and discussion

A microfluidic system with an integrated nanoporous membrane was successfully adapted for DNA extraction or sample preparation. A photograph of a complete device is shown in Fig. 2 along with a schematic showing the basic operation of the system. Note that once the molds are finished, the entire fabrication process can be completed within 30 min without using any photolithography, etchants or solvents.

One of the primary concerns related to the fabrication process was the bond strength between the PDMS, tape, and AOM. To verify the required bond strength, the bond failure pressure was measured using a dead end channel. At $586.05 \pm 34 \text{ kPa}$, the double side tape structure started to separate and leak between the tape and substrate. These bond strength results were better than published results for oxygen plasma bonding, which is usually used for PDMS-PDMS bonding and PDMS-glass bonding (maximum bond strength: 510.2 kPa).²⁰ The bond strength was clearly high enough to use in nearly any proposed application, including high-flow rate applications, as pressures in most microfluidic systems only occasionally exceed even 100 kPa.

The results of hgDNA collection and concentration on the AOM membranes with three different pore sizes embedded within microfluidic channels are summarized in Fig. 3, which shows the permeation rate through the membranes. A low permeation rate indicates that the hgDNA was captured on the membrane and not allowed to pass through the membrane. Note that these experiments were performed with hgDNA suspended in a buffer, not blood. For the no salt gDNA solutions, 80%, 20% and 0% of the initial amount of gDNA was permeated through the membranes with pore sizes of 200 nm, 100 nm and 20 nm, respectively (Fig. 3). The gDNA molecules are significantly larger than 200 nm and it was thought that pore size may have little impact on extraction, but this is clearly not the case. Pore size is likely not the only mechanism for extraction as it is likely there are electrostatic interactions (or salt bridges) between gDNA and hydroxyl group on the alumina, which will be discussed more later. Clearly the smaller pore sizes played a significant role in collecting the DNA and preventing its travel through the membrane when carried by a pressure driven flow. As the pore size decreased, the physical filtration effect and electrostatic interactions were sufficient to overcome any pressure or shear forces and allow the extraction of significantly more gDNA. Using the 20 nm membrane, most (if not all) of hgDNA was collected over the membrane. The question that remains is: will these small pores also be amenable for use with real samples, such as whole blood. Thus, it is important to note that both 100 nm and 200 nm pore sizes showed significant

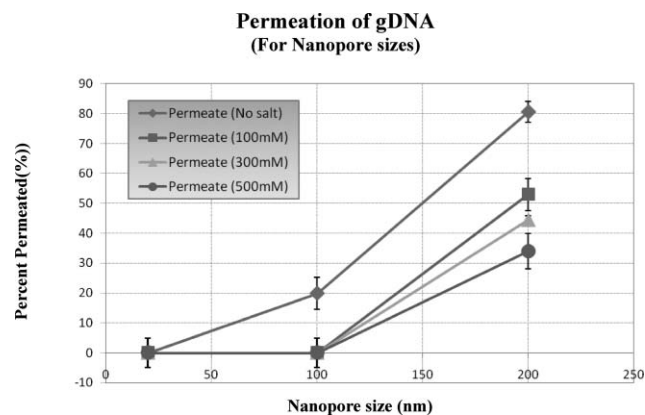


Fig. 3 DNA permeation rate through the AOMs depends on salt concentration. Higher salt concentrations lead to higher collection rates in all scenarios. Note that low permeation indicates a high collection rate.

ability for collecting and concentrating hgDNA, even if they did not perform as well as the 20 nm pore size membranes.

To understand the effect of salt concentration on gDNA collection over AOM membranes, the salt concentration was varied. As salt concentration increased, the capture rate for the 200 nm sized pores increased from 20% to 70%. Salt concentrations greater than 0.1 M caused 100% of the hgDNA to be captured in the 100 nm and 20 nm pore size membranes. The increased collection rate is thought to be due to the size, shape and aggregation state of the gDNA along with electrostatic interactions between the gDNA and the alumina. In high salt conditions, it is possible for gDNA to make a salt bridge with the alumina substrate which has many hydroxyl groups on the surface. Based on this binding effect, the collection rate depends on the amount of hydroxyl groups on the surface and the salt concentration. Another possible explanation of this result is charge neutralization of gDNA. As the salt concentration in the gDNA solution increases, the normally negatively charged (in solution) phosphate group of the DNA helix is neutralized and the overall charge of gDNA becomes neutral. At neutral charge, high concentrations of the multivalent/monovalent salt allows an attractive interaction between gDNA chains (or at least not a repulsive one) and eventually aggregation of the gDNA, which leads to larger gDNA complexes and better extraction.^{22,24} Thus, exposing the DNA molecules to a high salt concentration causes hgDNA to aggregate. Essentially, the apparent size of the molecules increases, causing an increase in the capture rate due to physical filtration effects. When charge density on the gDNA surface is reduced, though, the gDNA has a higher probability of non-specific adsorption to the nanoporous membrane. This can lead to other challenges though, as the non-specific adsorption of hgDNA can make it harder to detach the gDNA from the nanoporous membrane.

Based on the results of the experiments using previously purified DNA, hgDNA extraction tests were performed with whole blood samples. To use whole blood for testing, the blood cells have to be lysed under appropriate conditions. Protease K activity, which is affected by salt and Triton X-100 concentration as well as incubation at room temperature, is a critical factor in obtaining well lysed samples. Temperature and pH effects were minimized by using a standard protocol, but the salt concentration had to be controlled to manage the binding force of hgDNA on the membrane and to allow downstream PCR without inhibition. With prepared, lysed blood samples, hgDNA was extracted on the nanoporous membrane and eluted with different buffers to determine if lysis conditions and buffer type had any impact on DNA collection. Interestingly, in collecting gDNA, the Triton X-100 agent in the cell lysis buffer, a nonionic surfactant, made the membrane dewetting easy and decreased the flow resistance, decreasing the entire process time.

For the elution step, two buffers of different ionic strength were used based on the competing theories for hgDNA attachment to the alumina. With an anionic phosphate buffer it might be possible to displace the hgDNA from the membrane using an ion with a stronger affinity for the surface, which would also then provide a repulsive electrostatic force to keep the DNA off the surface. Another possibility is to use a cationic Tris buffer, to pull the DNA off the alumina surface. When the cationic buffer flows through the membrane, the hgDNA on the membrane dissolves

easily and detaches from the membrane surface. Also, to increase the repulsive force between the hgDNA and alumina surface, a pH 9 buffer solution was used. The point of zero charge (PZC) of the alumina membranes varies, but most of research result show the PZC value between 5–8.^{25–27} At a pH higher than the PZC, the alumina surface should be negatively charged and should help to increase the elution of gDNA. The extraction results of the lysis and elution tests using human blood samples are shown in Fig. 4. Using 200 nm pore membranes, less than 5% of the anticipated DNA was extracted from the whole blood sample. As previous test results showed, most of the particles within the lysed sample passed through the membrane without retention or absorption. Using the 100 nm and 20 nm pore membranes, two lysed samples (with and without salt) were used for a DNA extraction test and the eluted hgDNA quantified. The yield rate of the sample containing salt was lower than without salt. As mentioned before, the salt can increase the absorption and retention on the AOMs. To overcome these adsorption forces of the DNA, cationic and anionic buffer solutions were used and tested. Based on the result of these tests, it was determined that a cationic buffer provided a better yield than an anionic buffer. The displacement action of the anionic buffer was not enough to detach the hgDNA from the membrane surface. However, cationic buffer was able to dissolve the DNA off the membrane, increasing DNA yield. From these results it seems clear that cations (Na^+/K^+) are likely to limit binding to the membrane, both in the extraction phase and during the elution phase. Hydrogen ions (pH) did not affect the solution in quite the same way. In a basic solution (pH 9 for these experiments), aluminium oxide has a negative charge on the surface and the negative charge intensifies with an increase in the pH value,²⁸ resulting in electrostatic repulsion between the DNA and the alumina. This repulsive force also had an effect on the detachment of the hgDNA from the membrane, but does not appear to be dominant in this case.

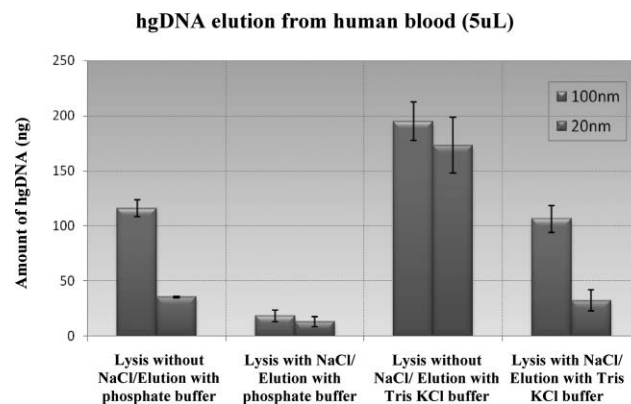


Fig. 4 Human genomic DNA extraction from whole blood samples. Different pore size membranes, lysis conditions and elution buffers were used to find the optimal conditions to maximize the DNA yield rate ($N = 5$).

An interesting feature of Fig. 4 relates to pore size effects. The 100 nm pores yielded more DNA than the 20 nm AOM. The mechanism for this result is not entirely clear. One possibility is that for the 100 nm pore AOM, more hgDNA was able to adsorb on to the aluminium oxide surface due to its greater contact area

(i.e. higher porosity/more surface). Another possibility is that the smaller pores clogged or were coated during the extraction process, limiting the amount of DNA that could be collected. Thus, the result could be from using a 'real' sample rather than using a purified DNA sample, as was the case with the results shown in Fig. 3. In either case, the results clearly showed a bias towards the 100 nm pore AOM. Overall, we determined that the best conditions for maximizing the DNA extraction rate is to use the 100 nm pore sized AOM, a low salt concentration during lysis and extraction, and a cationic elution buffer.

To show the suitability of the extracted DNA for further analysis, multiple target segments were PCR amplified. The hgDNA samples to be amplified were collected randomly from the exit of the microfluidic system. The PCR and DNA melting data for the CYP2C9*2 and VKORC1 genes on the extracted DNA are shown in Fig. 5. The target genes were well amplified and have identical melting curves when compared to results obtained with commercial kit. Based on these results, we have determined that the DNA is not heavily fragmented and it is possible to use the DNA for additional assays. The crossing points for the PCR data also provide some insight into the extraction capabilities of the system, and the concentration of the extracted DNA. The elution volume was 25 μl , and 5 μl samples were used for the PCR experiments. From Fig. 5, the concentrations of the eluted samples is clearly at least 5 $\text{ng } \mu\text{l}^{-1}$ and possibly a bit more. Since the eluted materials have been diluted five-fold, the measured concentration based on these PCR results would suggest an initial concentration of 25–35 $\text{ng } \mu\text{l}^{-1}$. As blood contains about 38 $\text{ng } \mu\text{l}^{-1}$, these results seem reasonable. It is possible that some of the DNA has not

fully been recovered from the membrane, and we have not done any studies to determine the maximum concentration that can be recovered (or the smallest volume to recover the DNA).

To test the quality of the eluted hgDNA sample, PCR inhibition was investigated by adding some of the extracted hgDNA to hgDNA sample purified with a commercial kit. If the hgDNA eluted from the microsystem has PCR inhibition factors in the mix, the crossing point of the real-time PCR curves should increase. As Fig. 6 shows, adding the hgDNA sample eluted from the microsystem has little impact on the observed PCR results. All of the samples (except the control) have nearly identical crossing points and the same melting point. These results suggest that the microfluidic DNA sample preparation system based on AOMs is an appropriate method for later integration with a PCR chip.

When compared to other microscale DNA extraction methods in the literature, the microfluidic sample preparation system demonstrated in this work was rapid (<10 min), required a small amount of blood volume (<10 μl), and the recovery ratio was dramatically enhanced. All system variations provided DNA that was amplified successfully and without any inhibition factors. These comparative results are summarized in Table 1.

Conclusions

To demonstrate a novel microfluidic DNA extraction system, AOMs were embedded with other microfluidic components to create a DNA sample preparation system. Based on the optimal conditions found using a pure DNA sample in the nanoporous hgDNA sample preparation system, the system was tested with

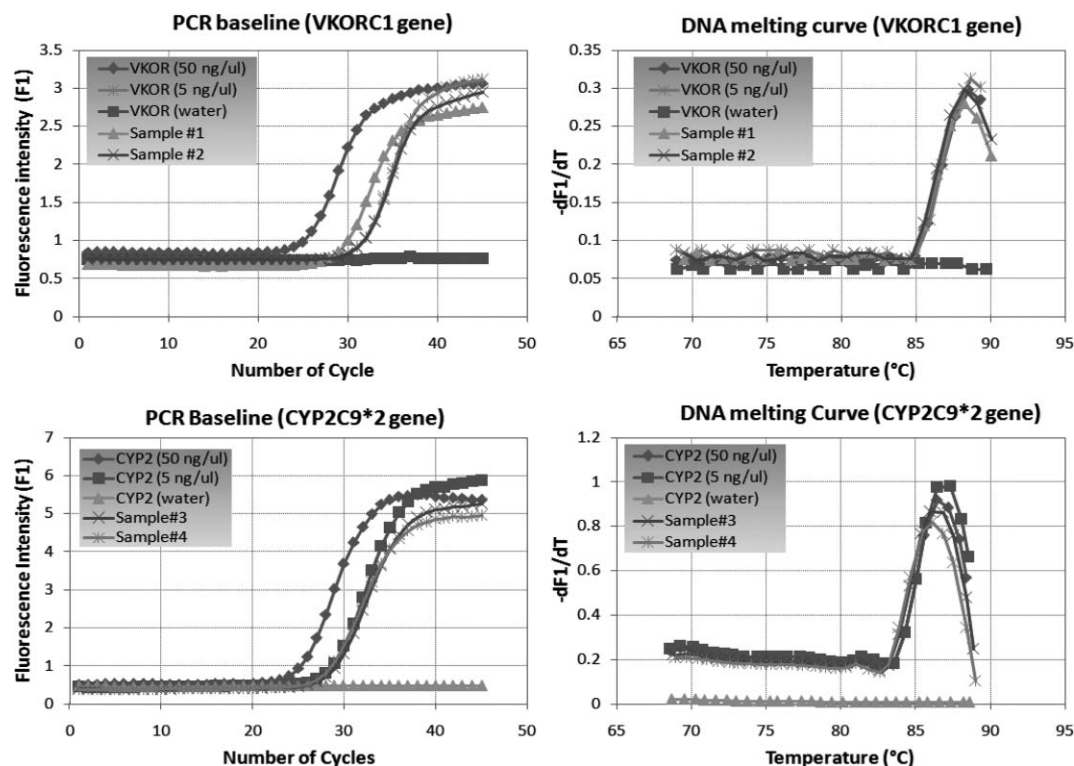


Fig. 5 PCR and DNA melting analysis was performed with hgDNA collected from the microfluidic extraction system. Two different locations were amplified (CYP2C9*2 and VKORC1). The melt curves verify that the correct segments were amplified.

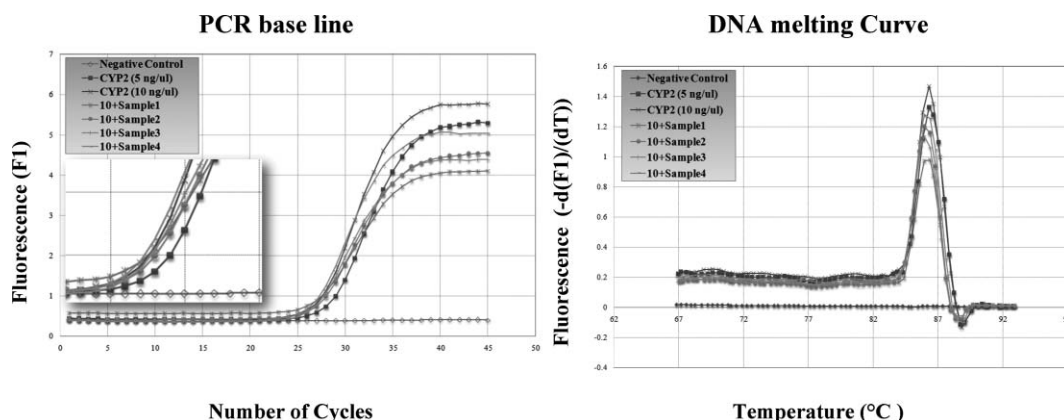


Fig. 6 A PCR inhibition test was performed with 10 parts of pre-purified gDNA ($10 \text{ ng } \mu\text{L}^{-1}$) and 1 part extracted gDNA from the microfluidic extraction system. Then, each sample was compared with different concentrations of purified DNA. Left, for the PCR baseline data, the C_p (crossing point) was about the same for each sample demonstrating that the eluted hgDNA contains no inhibition factors. Right, the melting temperature for each DNA sample was identical, suggesting that the same segment of DNA is amplified in each experiment.

Table 1 Comparison of microfluidic DNA sample preparation systems based on time, volume, recovery ratio, and amplifiability

Extraction method	Total time/min	Blood volume/ μL	Recovery/ $\text{ng } \mu\text{L}^{-1}$ of blood	PCR compatible	Ref.
Sol-gel silica bead	<57	10	28	Yes	13
Chitosan coating	<10	4	26	Yes	8
Aminosilane coated mag. bead	>25	5	20	Yes	9
Photopolymerized silica column	~30	2.5	34.9	Yes	15
Nanoporous membrane	<10	5	38.8	Yes	

lysed blood. The eluted hgDNA from the whole blood sample was amplified with a real-time PCR instrument. Among the 20 nm, 100 nm and 200 nm pore size membranes, the 100 nm pore size membrane had the highest yield of hgDNA from whole blood. The low salt concentration lysis solution and the cationic elution buffer positively impacted the extraction and elution of hgDNA. The eluted hgDNA sample was amplified at multiple locations without inhibition and had the correct melting curve. It appears that ionic interactions between cationic Tris buffer solution and the extracted hgDNA, along with the pressure-driven flow, overcame the binding forces between the hgDNA and the nanoporous membrane. Using the proposed AOM technology in an integrated microfluidic system, the sample preparation step can be simplified while reducing reagents and time compared to existing methods.

Acknowledgements

This research was supported by Synergy and TCP (Technology Commercialization Project) grants from the University of Utah. This research was also funded by the State of Utah Center of Excellence Program. We thank Niel Crews and Rajesh Surapaneni for help on the PCR experiments and useful discussions with Carl Wittwer's lab in support of the experiments.

References

- H. Tian, A. F. R. Huhmer and J. P. Landers, *Anal. Biochem.*, 2000, **283**, 175–191.
- K. A. Wolfe, M. C. Breadmore, J. P. Ferrance, M. E. Power, J. F. Conroy, P. M. Norris and J. P. Landers, *Electrophoresis*, 2002, **23**, 727–733.
- M. C. Breadmore, K. A. Wolfe, I. G. Arcibal, W. K. Leung, D. Dickson, B. C. Giordano, M. E. Power, J. P. Ferrance, S. H. Feldman, P. M. Norris and J. P. Landers, *Anal. Chem.*, 2003, **75**, 1880–1886.
- N. C. Cady, S. Stelick, M. V. Kunnakkam and C. A. Batt, *Sens. Actuators, B*, 2005, **107**, 332–341.
- H. H. Kessler, G. Mühlbauer, E. Stelzl, E. Daghofer, B. I. Santner and E. Marth, *Clin. Chem.*, 2001, **47**, 1124–1126.
- J. Pawliszyn, *Anal. Chem.*, 2003, **75**, 2543–2558.
- T. Nakagawa, T. I. Tanaka, D. Niwa, T. Osaka, H. Takeyama and T. Matsunaga, *J. Biotechnol.*, 2005, **116**, 105–111.
- W. Cao, C. J. Easley, J. P. Ferrance and J. P. Landers, *Anal. Chem.*, 2006, **78**, 7222–7228.
- T. Nakagawa, R. Hashimoto, K. Maruyama, T. Tanaka, H. Takeyama and T. Matsunaga, *Biotechnol. Bioeng.*, 2006, **94**, 864–868.
- J. Kim, K. V. Voelkerding, B. K. Gale, *Third IEEE-EMBS Special Conference on MMB*, Oahu, 2005.
- J. Kim, K. V. Voelkerding and B. K. Gale, *J. Micromech. Microeng.*, 2006, **16**, 33–39.
- M. G. Elgort, M. G. Herrmann, M. Erali, J. D. Durtschi, K. V. Voelkerding and R. E. Smith, *Clin. Chem.*, 2004, **50**, 1817–1819.
- Q. Wu, J. M. Bienvenue, B. J. Hassan, Y. C. Kwok, B. C. Giordano, P. M. Norris, J. P. Landers and J. P. Ferrance, *Anal. Chem.*, 2006, **78**, 5704–5710.
- M. A. Witek, S. D. Llopis, A. Wheatley, R. L. McCarley and S. A. Soper, *Nucleic Acids Res.*, 2006, **34**(e74), 71–79.
- J. Wen, C. Guillo, J. P. Ferrance and J. P. Landers, *Anal. Chem.*, 2006, **78**, 1673–1681.
- Product Guide 2005*, Whatman Laboratory, Div. 9, Bridewell Place, Clifton, NJ 07014, USA.
- D. A. Bartholomeusz, R. W. Boutté and J. D. Andrade, *IEEE J. Microelectromech. Syst.*, 2005, **14**, 1364–1374.
- A. M. Christensen, D. A. Chang-Yen and B. K. Gale, *J. Micromech. Microeng.*, 2005, **15**, 928–934.
- D. C. Duffy, J. C. McDonald, O. J. A. Schueller and G. M. Whitesides, *Anal. Chem.*, 1998, **70**, 4974–4984.
- S. Bhattacharya, A. Datta, J. M. Berg and S. Gangopadhyay, *IEEE J. Microelectromech. Syst.*, 2005, **14**, 590–597.

-
- 21 V. A. Bloomfield, *Biopolymers*, 1998, **44**, 269–282.
- 22 Y. Burak, G. Ariel and D. Andelman, *Biophys. J.*, 2003, **85**, 2100–2110.
- 23 S. K. Sia and G. M. Whitesides, *Electrophoresis*, 2003, **24**, 3563–3576.
- 24 Y. Burak, G. Ariel and D. Andelman, *Curr. Opin. Colloid Interface Sci.*, 2004, **9**, 53–58.
- 25 A. E. Ghzaoui, *J. Appl. Phys.*, 1999, **86**, 5894–5897.
- 26 D. Elzo, I. Huisman, E. Middelink and V. Gekas, *Colloids Surf., A*, 1998, **138**, 145–159.
- 27 M. Kosmulski, *J. Colloid Interface Sci.*, 2006, **298**, 730–741.
- 28 J. A. Schwarz and C. I. Contescu, *Surfaces of Nanoparticles and Porous Materials*, Marcel Dekker, New York, 1999.